scientific reports

Check for updates

OPEN

Experimental solubility and thermodynamic modeling of *empagliflozin* in supercritical carbon dioxide

Gholamhossein Sodeifian[1,2,3]✉, Chandrasekhar Garlapati[4], Fariba Razmimanesh[1,2,3] & Hassan Nateghi[1,2,3]

The solubility of *empagliflozin* in supercritical carbon dioxide was measured at temperatures (308 to 338 K) and pressures (12 to 27 MPa), for the first time. The measured solubility in terms of mole faction ranged from 5.14×10^{-6} to 25.9×10^{-6}. The cross over region was observed at 16.5 MPa. A new solubility model was derived to correlate the solubility data using solid–liquid equilibrium criteria combined with Wilson activity coefficient model at infinite dilution for the activity coefficient. The proposed model correlated the data with average absolute relative deviation (AARD) and Akaike's information criterion (AIC_c), 7.22% and − 637.24, respectively. Further, the measured data was also correlated with 11 existing (three, five and six parameters empirical and semi-empirical) models and also with Redlich-Kwong equation of state (RKEoS) along with Kwak-Mansoori mixing rules (KMmr) model. Among density-based models, Bian et al., model was the best and corresponding AARD% was calculated 5.1. The RKEoS + KMmr was observed to correlate the data with 8.07% (correspond AIC_c is − 635.79). Finally, total, sublimation and solvation enthalpies of *empagliflozin* were calculated.

List of symbols

A-D	New model constants
$A_1 - C_1$	Alwi–Garlapati model constants
$A_2 - C_2$	Bartle model constants
$A_3 - E_3$	Bian model constants
A_4 and B_4	Chrastil model constants
$A_5 - E_5$	Garlapati–Madras model constants
$A_6 - C_6$	Kumar–Johnstone model constants
$A_7 - C_7$	Mahesh–Garlapati model constants
$A_8 - C_8$	Mendez–Teja model constants
$A_9 - F_9$	Sodefian model constants
A_{10} and B_{10}	Reformulated Chrastil model constants
$A_{11} - F_{11}$	Tippana–Garlapati model constants
AARD	Absolute average relative deviation
Adj.R^2	Adjusted R^2
AIC	Akaike's information criterion
a_{ij}	EoS energy parameter
b_{ij}	EoS volume correction
C	Solubility in Chrastil model
C_p	Heat capacity
EoS	Equation of state
H_{sol}	Solvation enthalpy

[1]Department of Chemical Engineering, Faculty of Engineering, University of Kashan, Kashan 87317-53153, Iran. [2]Laboratory of Supercriritcal Fluids and Nanotechnology, University of Kashan, Kashan 87317-53153, Iran. [3]Modeling and Simulation Centre, Faculty of Engineering, University of Kashan, Kashan 87317-53153, Iran. [4]Department of Chemical Engineering, Puducherry Technological University, Puducherry 605014, India. ✉email: sodeifian@kashanu.ac.ir

H_{sub}	Sublimation enthalpy
H_{Total}	Total enthalpy
H_2^m	Melting enthalpy of the solute
Mscf	Molecular weight of supercritical fluid
N	Number of data points
P	Total pressure
P^{sub}	Sublimation pressure
RK	Redlich–Kwong
P_r	Reduced pressure
P_c	Critical pressure
Q	Number of parameters of a model
R	Universal gas constant
R^2	Square of correlation coefficient
RMSE	Root mean square deviation
SSE	Error sum of squares
T	Temperature
T_c	Critical temperature
T_m	Melting temperature
Tr	Reduced temperature
y_2	Solubility in molefraction

Greek symbols

Δ	Difference
$\hat{\varphi}_i^S$	Fugacity coefficient of the pure substance at saturation
$\hat{\varphi}_i^{ScCO_2}$	Solute fugacity in supercritical carbon dioxide ($ScCO_2$)
ϖ	Acentric factor
ρ	Density
ρ_r	Reduced density
κ_{ij}	EoS mixing rule parameter
l_{ij}	EoS mixing rule parameter
$\lambda_{12}, \lambda_{21}$	Wilson model parameters
γ_2^∞	Infinite dilution activity coefficient

Sub and superscripts

exp	Experimental
cal	Calculated
1	Solvent (CO_2)
2	Solute (drug)
c	Critical
m	Melting
r	Reduced

Supercritical carbon dioxide ($ScCO_2$) is a fluid above its critical point. It has physical properties (density, diffusivity, viscosity and surface tension) intermediate to that of gas and liquid[1,2]. $ScCO_2$ has been used as a solvent in various process applications, because it has gas like diffusivity and liquid like density with low viscosity and surface tension[1,3–5]. The major applications are in drug particle micronization, food processing, textile dyeing, ceramic coating, extraction and many more[4,6–12]. Although, several supercritical fluids are utilized as solvent in process industry, $ScCO_2$ is the most desirable solvent[8,13–17]. In general, phase equilibrium information is necessary to implement supercritical fluid technology (SFT)[6,7,9]. The solubility is the basic information for the design and development of SFT. In literature, solubility of many drug solids in $ScCO_2$ is readily available[18–30], however, the solubility of *empagliflozin* has not been reported, therefore in this work for the first time, its solubility in $ScCO_2$ has been measured. This data may be used in the particle micronization process using $ScCO_2$. The molecular formula of *empagliflozin* is $C_{23}H_{27}ClO_7$ and its molecular weight is 450.91. The chemical structure is shown in Fig. 1.

Empagliflozin is an inhibitor of sodium-glucose co-transporter-2 (SGLT2), the transporters primarily responsible for the re-absorption of glucose in the kidney. Further, it is useful in reducing the risk of cardiovascular death in adults with type 2 diabetes mellitus and cardiovascular disease[31]. Sufficient drug dosage is very essential for those treatments and this is achieved through a proper particle size. Therefore, the present study is quite useful in particle micronization using $ScCO_2$. Solubility measurement at each desired condition is very cumbersome and hence, there is a great need to develop a model that correlates/predicts the solubility[32]. Recent developments such as machine learning methods may be considered with the improvement of artificial intelligence prediction methods for the data correlation[33–35]. However, in general, the solubility models are classified into five types; however, only three are user friendly, and they are equation of state, density-based and mathematical models[36]. Directly or indirectly all of them are derived based on thermodynamic frame work. The derived models make use of the basic concepts related to phase equilibrium criteria (solid–gas or solid–liquid), solvent–solute association theory, dilute solution theory, solution theory and Wilson model or any other model[37]. In fact, most of the literature models correlate the solubility of the solid solutes in $ScCO_2$ quite well. A solid–gas equilibrium models need the

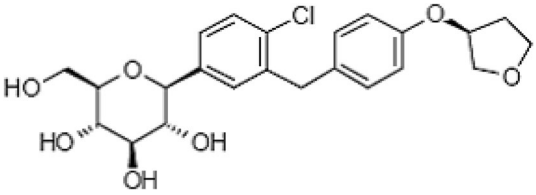

Figure 1. *Empagliflozin* chemical structure.

Compound	Formula	M_W (g/mol)	T_m (K)	λ_{max} (nm)	CAS number	Minimum purity by supplier
Empagliflozin	$C_{23}H_{27}ClO_7$	450.9	426.1	276	864070-44-0	99%
Carbon dioxide	CO_2	44.01			124-38-9	99.99%
DMSO	C_2H_6OS	78.13			67-68-5	99%

Table 1. Some physicochemical properties of the used materials.

critical properties and vapour pressure of the solute, while these properties are rarely available in literature, due to this, the group contribution methods are commonly used[38]. On the other hand, the solid–liquid equilibrium (SLE) criterion requires an appropriate model for activity coefficient calculation. A recent study reveals that SLE model in combination with Van Laar activity coefficient model can be a simple approach in model development, but this method resulted in an implicit expression in terms of mole fraction[38,39]. Therefore, there is a need to develop an explicit solubility model and hence, this task is taken up in this work.

The main motives of this study were in two levels. In the first level, *empagliflozin* solubility in $ScCO_2$ was determined and in the second level, a new explicit solubility model was developed based on solid–liquid equilibrium criterion in combination with Wilson activity coefficient model for the activity coefficient calculation.

Experimental

Materials. Gaseous CO_2 (purity > 99.9%) was obtained from Fadak company, Kashan (Iran), *empagliflozin* (CAS Number: 864070-44-0, purity > 99%) was purchased from Amin Pharma company, and dimethyl sulfoxide (DMSO, CAS No. 67-68-5, purity > 99%) was provided from Sigma Aldrich company. Table 1 indicates all the information about the chemicals utilized in this work.

Experiment details. The detailed discussion of the solubility apparatus and equilibrium cell has been presented in our earlier studies (Fig. 2)[19,25,40,41]. However, a brief description about the apparatus is presented in this section. This method may be classified as an isobaric-isothermal method[42]. Each measurement was carried out with high precision and temperatures and pressures were controlled within ± 0.1 K and ± 0.1 MPa, respectively. For all measurement, 1 g of *empagliflozin* drug was used. As mentioned in our previous works, the equilibrium was observed within 60 min. After equilibrium, 600 µL saturated $ScCO_2$ sample was collected via 2-status 6-way port valve in a DMSO preloaded vial. After discharging 600 µL saturated $ScCO_2$, the port valve was washed with 1 ml DMSO. Thus, the total saturation solution was 5 ml. Each measurement was repeated thrice and their average values were reported. Mole fraction is obtained as follows:

$$y_2 = \frac{n_{drug}}{n_{drug} + n_{CO_2}} \tag{1}$$

where n_{solute} is the moles number of the drug, and n_{CO_2} is the moles number of CO_2 in the sampling loop.

Further, the above quantities are given as:

$$n_{\text{solute}} = \frac{C_s \cdot V_s}{M_s} \tag{2}$$

$$n_{CO_2} = \frac{V_1 \cdot \rho}{M_{CO_2}} \tag{3}$$

where C_s is the drug concentration in saturated sample vial in g/L. The volume of the sampling loop and vial collection are $V_1(L) = 600 \times 10^{-6}$ m^3 and $V_s(L) = 5 \times 10^{-3}$ m^3, respectively. The M_s and M_{CO_2} are the molecular weight of drug and CO_2, respectively. Solubility is also described as

$$S = \frac{C_S V_s}{V_1} \tag{4}$$

The relation between S and y_2 is

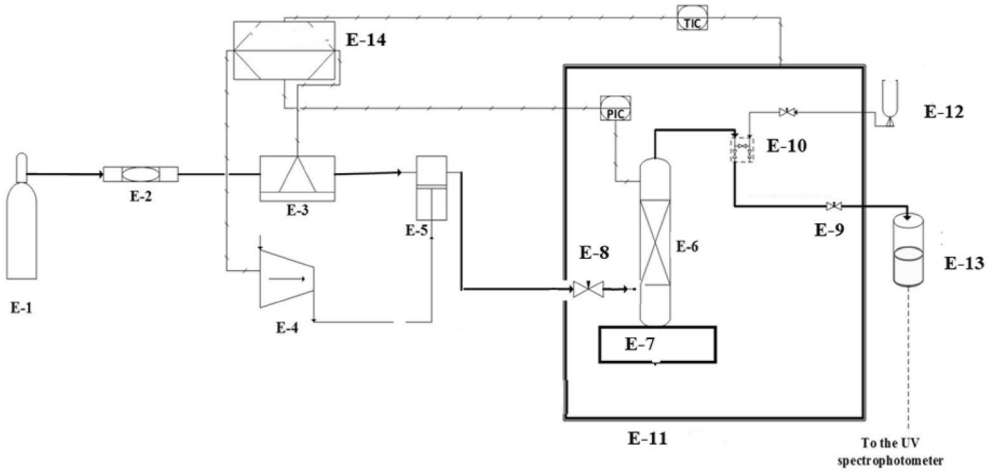

Figure 2. Experimental setup for solubility measurement, E1—CO_2 cylinder; E-2—Filter; E-3—Refrigerator unit; E-4—Air compressor; E-5—High pressure pump; E-6—Equilibrium cell; E-7—Magnetic stirrer; E-8—Needle valve; E-9—Back-pressure valve; E-10—Six-port, two position valve; E-11—Oven; E-12—Syringe; E13—Collection vial; E-14—Control panel.

$$S = \frac{\rho M_s}{M_{CO_2}} \frac{y_2}{1 - y_2} \tag{5}$$

A UV–Visible spectrophotometer (Model UNICO-4802) and DMSO solvent were used for the measurement of *empagliflozin* solubility. The samples were analyzed at 276 nm.

Existing and new models and their correlations

In this section, the details of various solubility models are presented along with a new explicit solubility model.

Existing models. *Alwi–Garlapati model (three parameters model)*[43]. It is one of the latest models for the solubility correlation. It is mathematically explained as

$$y_2 = \frac{1}{\rho_r T_r} \exp\left(A_1 + \frac{B_1}{T_r} + C_1 \rho_r\right) \tag{6}$$

where $A_1 - C_1$ are model constants.

Bartle et al., model (three parameters model)[44]. It is an empirical model and mathematically stated as:

$$\ln\left(\frac{y_2 P}{P_{ref}}\right) = A_2 + \frac{B_2}{T} + C_2(\rho - \rho_{ref}) \tag{7}$$

where $A_2 - C_2$ are model constants. From parameter B_2, one can estimate sublimation enthalpy using the relation, $\Delta_{sub}H = -B_2 R$, in which R is universal gas constant.

Bian et al., model (five parameters model)[45]. It is an empirical model and mathematically formulated as:

$$y_2 = \rho_1^{(A_3 + B_3 \rho_1)} \exp\left(C_3/T + D_3 \rho_1/T + E_3\right) \tag{8}$$

where $A_3 - E_3$ are model constants.

Chrastil model (three parameters model)[46]. It is a semi-empirical model and mathematically stated as:

$$c_2 = \rho_1^{\kappa} \exp\left(A_4 + \frac{B_4}{T}\right) \tag{9}$$

where κ, A_4 and B_4 are model constants.

In terms of mole fraction, it is written as[47]:

$$y_2 = \frac{(\rho_1)^{\kappa-1} \exp\left(A_4 + \frac{B_4}{T}\right)}{\left[1 + (\rho_1)^{\kappa-1} \exp\left(A_4 + \frac{B_4}{T}\right)\right]} \tag{9a}$$

Garlapati–Madras model (five parameters model)[48]. It is a mathematical model and mathematically formulated as

$$\ln\left(y_2\right) = A_5 + (B_5 + C_5\rho_1)\ln\left(\rho_1\right) + \frac{D_5}{T} + E_5 \ln\left(\rho_1 T\right) \tag{10}$$

where $A_5 - E_5$ are model constants.

Kumar–Johnstone model (three parameters model)[49]. It is a semi empirical model and mathematically described as:

$$\ln\left(y_2\right) = A_6 + B_6\rho + C_6/T \tag{11}$$

where $A_6 - C_6$ are model constants.

Mahesh–Garlapati model (three parameters model)[39]. It is one of the latest models. It is based on degree of freedom and mathematically stated as:

$$\ln\left(y_2\right) = A_7 + B_7\rho_r T_r + C_7\rho_r T_r^3 \tag{12}$$

where $A_7 - C_7$ are model constants.

Mendez–Teja model (three parameters model)[50]. It is a semi-empirical model and mathematically explained as:

$$T\ln\left(y_2 P\right) = A_8 + B_8\rho + C_8 T \tag{13}$$

where $A_8 - C_8$ are model constants.

Sodefian et al., model (six parameters model)[40]. It is a mathematical model and stated as:

$$\ln\left(y_2\right) = A_9 + \frac{B_9 P^2}{T} + C_9 \ln\left(\rho_1 T\right) + D_9(\rho_1 \ln\left(\rho_1\right)) + E_9 P \ln\left(T\right) + F_9\frac{\ln\left(\rho_1\right)}{T} \tag{14}$$

where $A_9 - F_9$ are model constants.

Reformulated Chrastil model (three parameters model)[47,51]. It is a semi-empirical model and mathematically explained as:

$$y_2 = \left(\frac{RT\rho_1}{M_{CF}f^{\cdot}}\right)^{\kappa'-1} \exp\left(A_{11} + \frac{B_{11}}{T}\right) \tag{15}$$

where κ', A_{10} and B_{10} are model constants.

Tippana–Garlapati model (six parameters model)[52]. It is a degree of freedom model and mathematically stated as:

$$y_2 = \left(A_{12} + B_{11}P_r + C_{11}P_r^2\right)T_r^2 + \left(D_{11} + E_{11}P_r + F_{11}P_r^2\right) \tag{16}$$

where $A_{11} - F_{11}$ are model constants.

New model. According to solid–liquid phase equilibrium criteria, the fugacity of the solute in the solid phase and liquid phase is equal at equilibrium. The liquid phase is considered as an expanded liquid phase of $ScCO_2$. At equilibrium, the solubility may be expressed as[53–57]

$$y_2 = \frac{1}{\gamma_2^{\infty}}\frac{f_2^S}{f_2^L} \tag{17}$$

where γ_2^{∞} is drug activity coefficient at infinitesimal dilution in $ScCO_2$ and f_2^S and f_2^L are fugacities of drug in the solid and $ScCO_2$ phases, respectively. The f_2^S/f_2^L ratio may be expressed as follows:

$$\ln\left(\frac{f_2^S}{f_L^L}\right) = \frac{\Delta H_2^m}{RT}\left(\frac{T}{T_m} - 1\right) - \int_{T_m}^{T}\frac{1}{RT^2}\left[\int_{T_m}^{T}\left[\Delta C_p\right]dT\right]dT \tag{18}$$

where,ΔC_p is heat capacity difference of the drug in solid phase and that of $SCCO_2$ phase. The terms that include ΔCp is much smaller than the term that has ΔH_2^m[58], thus leaving ΔCp term yields a much simpler expression for fugacity ratio as:

$$\ln\left(\frac{f_2^S}{f_L^L}\right) = \frac{\Delta H_2^m}{RT}\left(\frac{T}{T_m} - 1\right) \tag{19}$$

Combining Eq. (19) with Eq. (17) give the expression for the solubility model (Eq. (20)).

$$y_2 = \frac{1}{\gamma_2^\infty}\exp\left[\frac{\Delta H_2^m}{RT}\left(\frac{T}{T_m} - 1\right)\right] \tag{20}$$

In order to use Eq. (20), the appropriate model for γ_2^∞ is essential.

In this work, the required activity coefficient is obtained from Wilson activity coefficient model[56] at infinite dilution and it is given by the Eq. (21).

$$\gamma_2^\infty = \exp\left[-\ln(\lambda_{21}) + 1 - \lambda_{12}\right] \tag{21}$$

where $\lambda_{12} = (V_2/V_1)\exp(-a_{12}/RT)$ and $\lambda_{21} = (V_1/V_2)\exp(-a_{21}/RT)$, V_1 and V_2 are molar volumes of solvent and solute, respectively.

When $\rho_1 = 1/V_1$, the final expression for the infinite dilution activity coefficient is obtained as:

$$\gamma_2^\infty = \exp\left[1 + \ln(\rho_1 V_2) + \frac{a_{21}}{RT} - \rho_1 V_2 \exp\left(\frac{-a_{12}}{RT}\right)\right] \tag{22}$$

The quantities a_{12} and a_{21} are assumed to be functions of reduced solvent density[57], and molar volume of the solute is assumed as a constant value. In this work, a_{12} and a_{21} are assumed to have the following form:

$$a_{12} = A(\rho_r)^B \tag{23}$$

$$a_{21} = C(\rho_r)^D \tag{24}$$

Combining Eqs. (22), (23) and (24) with Eq. (20), give the following new explicit solubility model:

$$y_2 = \exp\left[\frac{\Delta H_2^m}{RT}\left(\frac{T}{T_m} - 1\right)\right] / \exp\left[1 + \ln(\rho_1 V_2) + \frac{A(\rho_r)^B}{RT} - \rho_1 V_2 \exp\left(\frac{-C(\rho_r)^D}{RT}\right)\right] \tag{25}$$

Equation (25) has four temperature independent adjustable variables namely *A*,*B*,*C* and *D*.

Equation of state (EoS) model. The solubility of drug *i* (solute) in $ScCO_2$ (solvent) is expressed as[59–61]:

$$\mathrm{y_i} = \frac{P_i^S \hat{\varphi}_i^S}{P\hat{\varphi}_i^{ScCO_2}}\exp\left[\frac{(P - P_i^S)V_S}{RT}\right] \tag{26}$$

where P_i^s is the sublimation pressure of the pure solid at system temperature T, P is the system pressure,V_s is the molar volume of the pure solid, *R* is the universal gas constant. The fugacity coefficient of the pure solute at saturation ($\hat{\varphi}_i^S$) is usually taken to be unity. In this work, the fugacity coefficient of the solute in the supercritical phase $\hat{\varphi}_i^{ScCO_2}$ is calculated using EoS along with KMmr[57]. The expression used for calculation of $\hat{\varphi}_i^{ScCO_2}$ is obtained from the following basic thermodynamic relation[60]:

$$\ln\left(\hat{\varphi}_i^{ScCO_2}\right) = \frac{1}{RT}\int_v^\infty\left[\left(\frac{\partial P}{\partial N_i}\right)_{T,V,N_j} - \frac{RT}{v}\right]dv - \ln Z \tag{27}$$

The expression for $\hat{\varphi}_i^{ScCO_2}$ is

$$\begin{aligned}\ln\left(\hat{\varphi}_i^{ScCO_2}\right) = {} & \ln\left(\frac{v}{v-b}\right) + \left(\frac{2\sum x_j b_{ij} - b}{v-b}\right) - \ln(Z) \\ & + \left(\frac{a\left(2\sum x_j b_{ij} - b\right)}{b^2 RT^{3/2}}\right)\left[\ln\left(\frac{v+b}{v}\right) - \frac{b}{v+b}\right] \\ & \left(3\alpha^{1/2}\left(\sum x_j a_{ij}^{2/3} b_{ij}^{1/3}\right)/b^{1/2} - \alpha^{2/3}\left(\sum x_j b_{ij}/b^{3/2}\right)\right)/bRT^{3/2}\end{aligned} \tag{28}$$

where $\alpha = \sum_i^n \sum_j^n x_i x_j a_{ij}^{2/3} b_{ij}^{1/3}$

and the associated mixing rules are:

$$a = \frac{\left(\sum_i^n \sum_j^n x_i x_j a_{ij}^{2/3} b_{ij}^{1/3}\right)^{3/2}}{\left(\sum_i^n \sum_j^n x_i x_j b_{ij}^{1/2}\right)^{1/2}} \tag{29}$$

$$b = \sum_i^n \sum_j^n x_i x_j b_{ij} \tag{30}$$

$$a_{ij} = \left(1 - k_{ij}\right)\sqrt{a_{ii} a_{jj}} \tag{31}$$

$$b_{ij} = \left(1 - l_{ij}\right)\frac{\left(b_{ii}^{1/3} + b_{jj}^{1/3}\right)^3}{8} \tag{32}$$

The main reason for considering RKEoS is that it has only two adjustable constants k_{ij} and l_{ij}.
All the models (density-based, new and RKEoS models) are correlated with the following objective function[58]:

$$OF = \sum_{i=1}^{N} \frac{\left|y_{2i}^{\exp} - y_{2i}^{calc}\right|}{y_{2i}^{\exp}} \tag{33}$$

The regression ability of a model is indicated in terms of an average absolute relative deviation percentage (AARD %).

$$\text{AARD (\%)} = (100/N_i) \sum_{i=1}^{N} \frac{\left|y_{2i}^{\exp} - y_{2i}^{cal}\right|}{y_{2i}^{\exp}} \tag{34}$$

For the regression, fminsearch (MATLAB 2019a®) algorithm has been used.

Results and discussion

Table 1 shows some physicochemical properties of the used materials. *Empagliflozin* solubility in $ScCO_2$ is reported at various temperatures (T = 308 to 338 K) and pressures (P = 12 to 27 MPa). Table 2 indicates the solubility data and $ScCO_2$ density. The reported $ScCO_2$ density is obtained from the NIST data base. Figure 3 shows the effect of pressure on various isotherms. The cross over region is observed at 16.5 MPa. From Fig. 3, below the cross over region, solubility decreases with increase in temperature, and on the other hand, above the cross over region, the solubility increases with increase in temperature. The EoS model requires critical properties which are computed with standard group contribution methods based on the chemical structure[62–65]. The summary of the critical properties computed are shown in Table 3. Figure 4 presents the self-consistency of the measured data with MT model.

The density-based models considered in this work have different number of adjustable parameters. These parameters range from three to six numbers. The regression results of all the models are indicated in Tables 4 and 5. The correlating ability of the models is depicted in Figs. 5, 6, 7, 8, 9, 10, 11. From the results, it is clear that all the models are able to correlate the data reasonably well and maximum AARD% is observed to be 10.4%. It is believed that, more parameter models are able to correlate the data more accurately. Sodefian et al., model is able to correlate the data with AARD = 5.84% and Akaike's information criterion (AIC = − 637.59) (more relevant information is presented in the following section). Among density models, Bian et al., model (five parameters model) is able to correlate the data well and corresponding AARD% is 5.1%. Interestingly, Chrastil (three parameters model) and Reformulated Chrastil models (three parameters model) are also able to correlate the data quite well. Further, Chrastil and Reformulated Chrastil models are able to provide the total enthalpy. Whereas, Bartle et al., model parameters are able to provide sublimation enthalpy of the *empagliflozin* drug. From the magnitude difference between the total and sublimation enthalpies, a solvation enthalpy is calculated. These results are reported in Table 6.

A new explicit solubility model based on solid–liquid equilibrium criteria combined with Wilson activity coefficient model corresponding to infinitesimal dilution is derived. The new model has four parameters *A*, *B*, *C* and *D*. While regression, new model parameters are treated as temperature independent and solid molar volume is kept constant. The new model requires melting point, melting enthalpy and molar volume of *empagliflozin* drug, and these values are obtained from literature and group contribution methods. From literature[31], the melting point of *empagliflozin* drug (426.1 K), molar volume (3.2699×10^{-4} m^3/mol) and melting enthalpy (60.238 kJ/mol) are calculated based on literature, Immirzi and Perini[63] and Jain et al., methods[66], respectively. The new model makes use of objective function given in Eq. (33). Similarly, RKEoS along KMmr correlations are established with the help of critical properties given in Table 3 (temperature independent correlations). The optimization results of the new solubility and RKEoS models are indicated in Table 5.

In order to examine the ability of models for correlating the solubility data, AIC is applied[67–70]. When the data number is less than < 40, the corrected AIC (AIC_c) is used.

Temperature (K)[a]	Pressure (MPa)[a]	Density of $ScCO_2$ (kg/m^3)[71]	$y_2 \times 10^4$ (mole fraction)	Experimental standard deviation, $S(\bar{y}) \times (10^4)$	S (equilibrium solubility) (g/L)	Expanded uncertainty of mole fraction (10^4U)
308	12	769	0.0814	0.0021	0.0643	0.0055
	15	817	0.1266	0.0042	0.1060	0.0098
	18	849	0.1327	0.0010	0.1156	0.0062
	21	875	0.1411	0.0051	0.1265	0.0118
	24	896	0.1501	0.0063	0.1378	0.0137
	27	914	0.1806	0.0071	0.1692	0.0161
318	12	661	0.0706	0.0023	0.0479	0.0052
	15	744	0.1182	0.0031	0.0901	0.0081
	18	791	0.1515	0.0032	0.1228	0.0091
	21	824	0.1601	0.0041	0.1353	0.0107
	24	851	0.2040	0.0064	0.1812	0.0151
	27	872	0.2079	0.0093	0.1858	0.0202
328	12	509	0.0611	0.0031	0.0319	0.0066
	15	656	0.1044	0.0023	0.0702	0.0062
	18	725	0.1620	0.0032	0.1203	0.0094
	21	769	0.1860	0.0042	0.1467	0.0115
	24	802	0.2248	0.0091	0.1849	0.0206
	27	829	0.2260	0.0021	0.1920	0.0107
338	12	388	0.0514	0.0023	0.0204	0.0047
	15	557	0.0928	0.0011	0.0530	0.0047
	18	652	0.2002	0.0101	0.1338	0.0219
	21	710	0.2266	0.0112	0.1650	0.0242
	24	751	0.2637	0.0103	0.2030	0.0231
	27	783	0.2590	0.0091	0.2079	0.0213

Table 2. Solubility of crystalline *empagliflozin* in $ScCO_2$ at various temperatures and pressures. The experimental standard deviation was obtained by $S(y_k) = \sqrt{\frac{\sum_{j=1}^{n}(y_j-\bar{y})^2}{n-1}}$. Expanded uncertainty $(U) = k^* u_{combined}$ and the relative combined standard uncertainty $u_{combined}/y = \sqrt{\sum_{i=1}^{N}(P_i u(x_i)/x_i)^2}$ [a]Standard uncertainty u are u(T) = ± 0.1 K; u(p) = ± 0.1 MPa. The value of the coverage factor k = 2 was chosen on the basis of the level of confidence of approximately 95 percent.

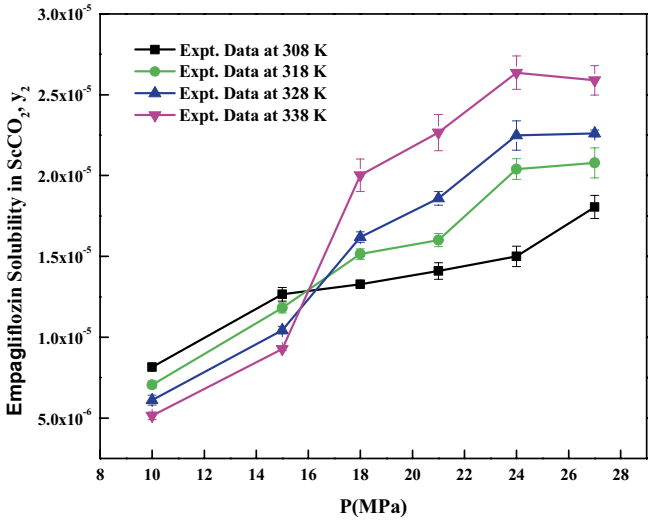

Figure 3. *Empagliflozin* solubility in $ScCO_2$ vs. pressure.

Substance	T_c (K)	P_c(Pa)	ω	$V^s \times 10^{-6}$ (m^3/mol)	T(K)			
					P_{sub} (Pa)[e]			
					308	318	328	338
Empagliflozin	870.367[a]	18.7565[b]	0.479[c]	184.397[d]	0.0034	0.0089	0.022	0.0508
CO_2	304.18	73.8	0.225					

Table 3. Critical and physical properties of *empagliflozin* and CO_2. T_c: critical temperature; P_c: critical pressure; ω: acentric factor; V^s: solid molar volume; T: temperature. [a]Estimated by Fedors method. [b]Estimated by the Joback and Reed method. [c]Estimated by Lee-Kesler vapour pressure relations (the required normal boiling temperature (at 1.0 atm), T_b is estimated with Klincewicz relation, $T_c = 50.2–0.16\ M + 1.41\ Tb$, where M is molecular weight). [d]Estimated by Immirzi, A., Perini, B method. [e]Estimated by Lee-Kesler vapour method.

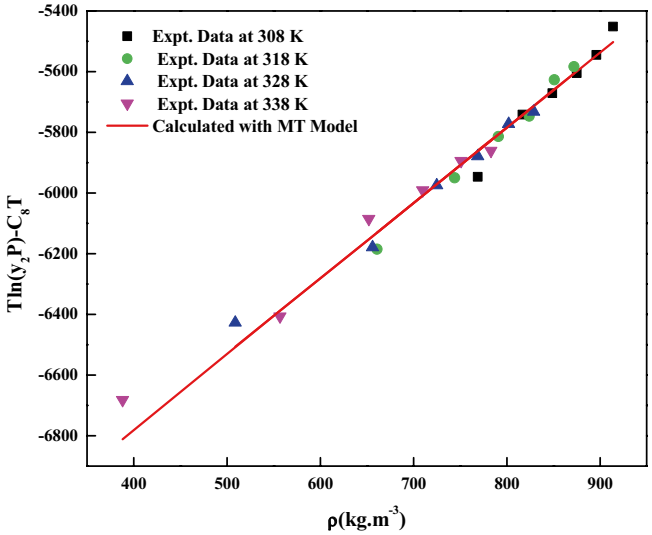

Figure 4. Self-consistency plot based on MT model.

Name of the empirical model	Correlation parameters	AARD%	R^2	R^2_{adj}
Alwi–Garlapati model	$A_1 = -1.8293$; $B_1 = -14.218$; $C_1 = 2.8519$	6.58	0.941	0.932
Bartle et al., model	$A_2 = 12.195$; $B_2 = -5972.3$; $C_2 = 7.7336 \times 10^{-3}$	10.4	0.922	0.910
Bian et al., model	$A_3 = -0.062205$; $B_3 = -5.7629 \times 10^{-4}$; $C_3 = -6230.8$; $D_3 = 2.9473$; $E_3 = 4.5582$	5.1	0.951	0.938
Chrastil model	$\kappa = 3.9083$; $A_4 = -18.97$; $B_4 = -3674.3$	9.21	0.943	0.934
Garlapati–Madras model	$A_5 = -750.2$; $B_5 = 852.82$; $C_5 = 1.0855$; $D_5 = -7397.7$; $E_5 = -11.163$	7.09	0.946	0.930
Kumar–Jonstone model	$A_6 = -14.274$; $B_6 = -0.53652$; $C_6 = 2.1216$	27.3	0.902	0.892
Mahesh_Garlapati model	$A_7 = -14.266$; $B_7 = -0.52714$; $C_7 = 2.0972$	8.14	0.931	0.921
Mendez–Teja model	$A_8 = -7775.4$; $B_8 = 2.3557$; $C_8 = 12.694$	9.95	0.924	0.912
Sodefian et al., model	$A_9 = -23.94$; $B_9 = 1.6043 \times 10^{-3}$; $C_9 = 2.4939$; $D_9 = 2.6639 \times 10^{-4}$; $E_9 = -9.5238 \times 10^{-3}$; $F_9 = -1.037 \times 10^3$	5.84	0.956	0.940
Reformulated Chrastil model	$\kappa' = 3.8748$; $A_{10} = -33.58$; $B_{10} = -2705.8$	9.14	0.943	0.935
Tippana–Garlapati model	$A_{11} = -6.4027 \times 10^{-5}$; $B_{11} = -1.1813 \times 10^{-5}$; $C_{11} = 2.0367 \times 10^{-5}$; $D_{11} = 4.4544 \times 10^{-5}$; $E_{11} = 3.5989 \times 10^{-5}$; $F_{11} = -2.4670 \times 10^{-5}$	6.63	0.927	0.924

Table 4. Correlation constants for the exiting empirical models.

Model	Correlation parameters	AARD%	R^2	R^2_{adj}
New model	A = 36,634; B = − 0.096039; C = − 9673.6; D = − 0.16480	7.22	0.949	0.941
RKEoS + Kwak Mansoori mixing rule model	$k_{ij} = 0.32061$; $l_{ij} = 0.1949$	8.07	0.951	0.946

Table 5. Calculated result for the new model and RKEoS + Kwak-Mansoori mixing rule model.

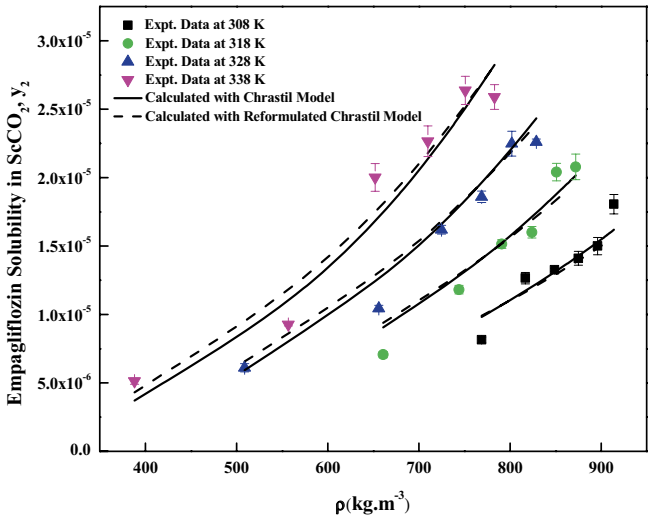

Figure 5. *Empagliflozin* solubility vs. $ScCO_2$ density. Solid lines and broken lines are calculated solubilities with Chrastil and Reformulated Chrastil models, respectively.

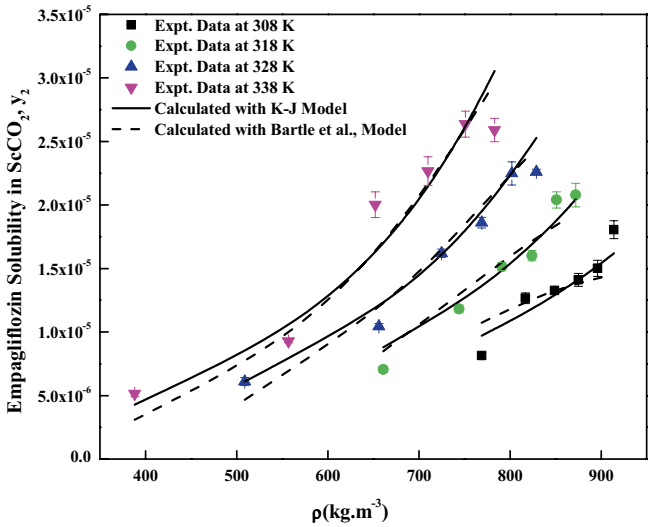

Figure 6. *Empagliflozin* solubility vs. $ScCO_2$ density. Solid lines and broken lines are calculated solubilities with KJ and Bartle et al., models, respectively.

$$AIC_c = AIC + \frac{2Q(Q+1)}{N-Q-1} \tag{35}$$

where AIC, N, Q and SSE are $N \ \ln(SSE/N) + 2Q$, the number of observations, the number of adjustable parameters of the model and the error sum of squares, respectively. According to AIC_c criterion, the best model has the least AIC_c value. Table 7 shows AIC_c values for various models considered in this study. In terms of AIC_c, all the models are able to correlate the data closely. However, Reformulated Chrastil model has AIC_c value (− 637.02), hence it is treated as the best model and at the same time, Tippana–Garlapati model has the highest AIC_c value (− 621.69), therefore, it is considered as a poorly correlating model. Three parameters models namely Chrastil, Alwi–Garlapati and Mendez–Teja models have AIC_c values − 636.95, − 635.3 and − 635.4, respectively. The new model which has four parameters, indicating comparable performance with the best model (AIC_c value of − 637.24).

Conclusion

Solubilities of *empagliflozin* in $ScCO_2$ at temperatures (T = 308–338 K) and pressures (P = 12–27 MPa) were reported for the first time. The measured solubility in terms of mole faction ranged from 5.14×10^{-6} to 25.9×10^{-6}. The data was successfully correlated with several models, Bian et al., model (AARD = 5.1%) was observed to be the best model in correlating the solubility data. All the models are able correlate the data reasonable. However,

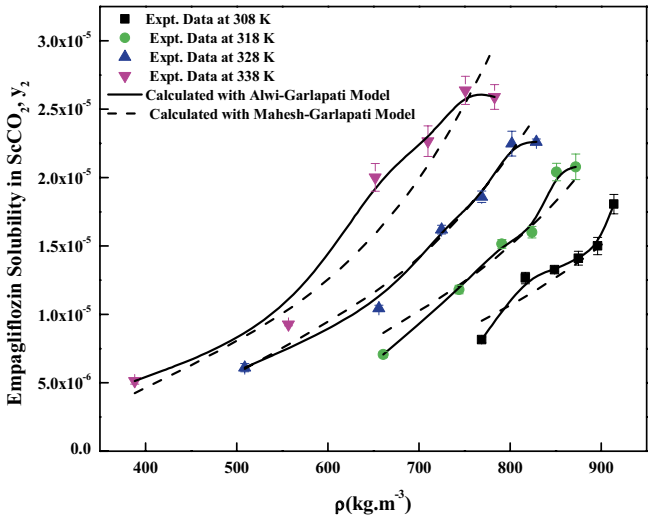

Figure 7. *Empagliflozin* solubility vs. $ScCO_2$ density. Solid lines and broken lines are calculated solubilities with Alwi–Garlapati and Mahesh–Garlapati models, respectively.

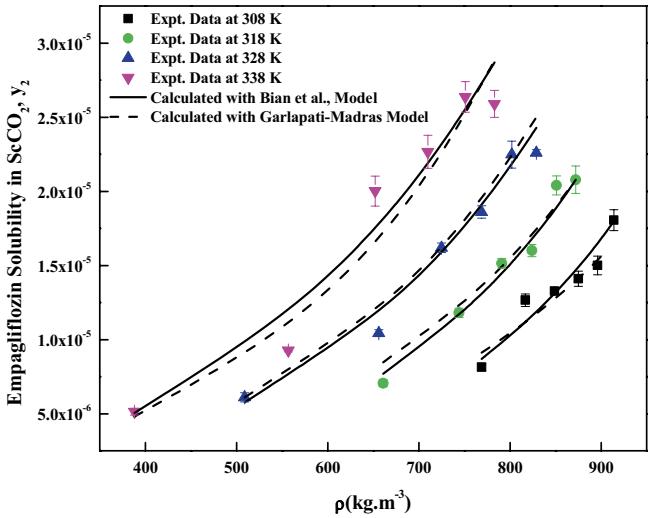

Figure 8. *Empagliflozin* solubility vs. $ScCO_2$ density. Solid lines and broken lines are calculated solubilities with Bian et al., and Garlapati–Madras models, respectively.

the correlating ability in ascending order of various models in terms of the lowest AIC_c values is as follows: Bian et al., Reformulated Chrastil, Chrastil, new solid–liquid equilibrium, Mendez–Teja, RKEoS + KMmr, Alwi–Garlapati, Sodefian et al., Mahesh–Garlapati, Bartle et al., Tippana–Garlapati models. The new model proposed in this work may be useful for correlating solids solubility in any SCF.

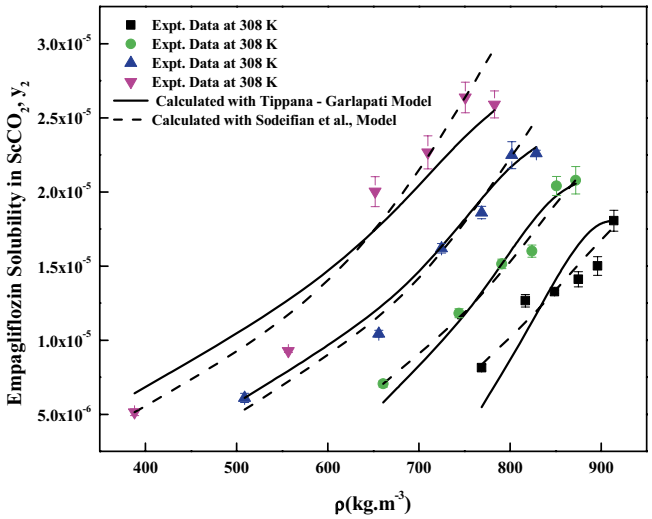

Figure 9. *Empagliflozin* solubility vs. $ScCO_2$ density. Solid lines and broken lines are calculated solubilities with Tippana–Garlapati and Sodeifian et al., models, respectively.

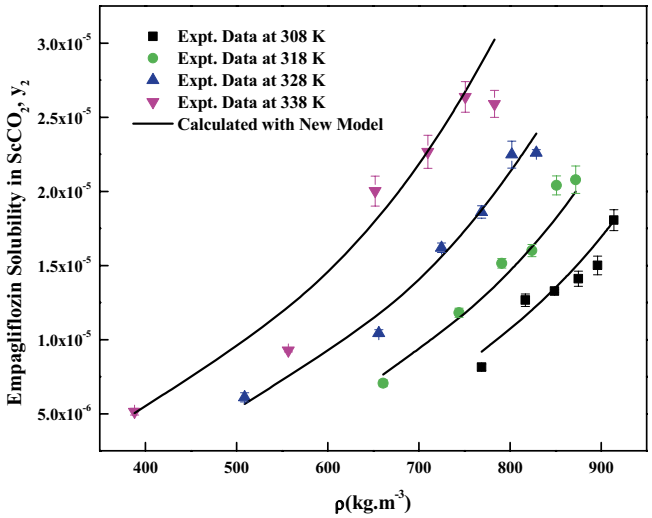

Figure 10. *Empagliflozin* solubility vs. $ScCO_2$ density. Solid lines are calculated solubilities with new model.

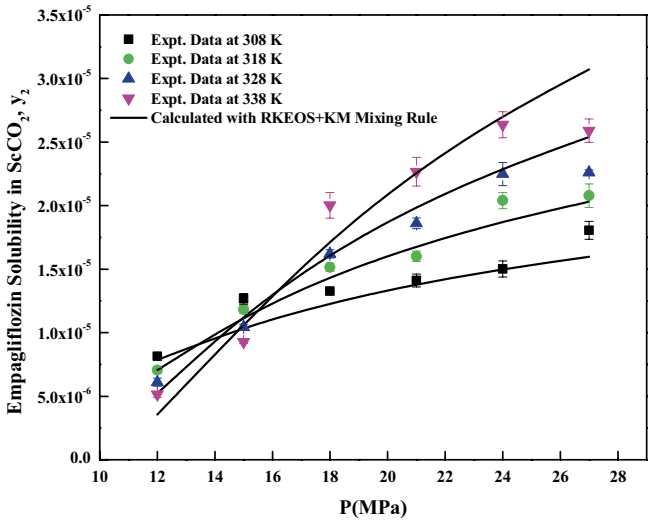

Figure 11. *Empagliflozin* solubility vs. pressure. Solid lines are calculated solubilities with RKEoS + KM mixing rule.

Model	Thermodynamic property		
	Total entalpy, ΔH_{total} (kJ/mol)	Enthalpy of sublimation, ΔH_{sub} (kJ/mol)	Enthalpy of solvation, ΔH_{sol} (kJ/mol)
Chrastil model	30.548[a]		− 19.105[d]
Reformulated Chrastil model	22.496[b]		− 27.157[e]
Bartle et al., model		49.653[c] (approximate value)	

Table 6. Computed thermodynamic properties. [a]Obtained with Chrastil model [b]Obtained with Reformulated Chrastil model [c]Obtained with Bartle et al. [d]Obtained as a result of difference between the $\Delta H_{sub}{}^{c}$ and $\Delta H_{total}{}^{a}$. [e]Obtained as a result between the $\Delta H_{sub}{}^{c}$ and $\Delta H_{total}{}^{b}$.

Model	SSE.10^{11}	RMSE.10^{6}	N	Q	AIC	AIC_c
Existing density models						
Alwi–Garlapati model	5.673	1.537	3	24	− 636.5	− 635.30
Bartle et al., model	7.391	1.755	3	24	− 630.15	− 628.95
Bian et al., model	4.338	1.345	5	24	− 638.94	− 635.6
Chrastil model	5.297	1.486	3	24	− 638.15	− 636.95
Garlapati–Madras model	4.828	1.418	5	24	− 636.37	− 633.04
Kumar–Jonstone model	6.537	1.650	3	24	− 633.1	− 631.9
Mahesh_Garlapati model	6.337	1.625	3	24	− 633.84	− 632.64
Mendez–Teja model	5.650	7.51	3	24	− 636.60	− 635.4
Sodefian et al., model	4.222	1.326	6	24	− 637.59	− 632.65
Reformulated Chrastil model	5.280	1.483	3	24	− 638.22	− 637.02
Tippana–Garlapati model	6.659	1.666	6	24	− 627.0	− 621.69
New model						
New solid–liquid equilibrium model	4.635	1.389	4	24	− 639.35	− 637.24
EoS model						
RKEoS model + Kwak-Mansoori mixing rule	6.201	1.607	2	24	− 636.36	− 635.79

Table 7. Statistical quantities (SSE, RMSE, AIC and AIC_c) of various models.

Data availability

The datasets generated and/or analysed during the current study are not publicly available due to confidential cases are available from the corresponding author on reasonable request.

Received: 16 March 2022; Accepted: 16 May 2022
Published online: 30 May 2022

References

1. Akgerman, A. & Madras, G. *Supercritical Fluids: Fundamentals and Applications* (Kluwer Academic, 1994).
2. Sodeifian, G., Razmimanesh, F. & Sajadian, S. A. Prediction of solubility of sunitinib malate (an anti-cancer drug) in supercritical carbon dioxide ($SC–CO_2$): Experimental correlations and thermodynamic modeling. *J. Mol. Liq.* **297**, 111740 (2020).
3. Hitchen, S. & Dean, J. Properties of supercritical fluids. In *Applications of Supercritical Fluids in Industrial Analysis* 1–11 (Springer, 1993).
4. Subramaniam, B., Rajewski, R. A. & Snavely, K. Pharmaceutical processing with supercritical carbon dioxide. *J. Pharm. Sci.* **86**(8), 885–890 (1997).
5. Sodeifian, G., Razmimanesh, F., Sajadian, S. A. & Hazaveie, S. M. Experimental data and thermodynamic modeling of solubility of Sorafenib tosylate, as an anti-cancer drug, in supercritical carbon dioxide: Evaluation of Wong-Sandler mixing rule. *J. Chem. Thermodyn.* **142**, 105998 (2020).
6. Bahrami, M. & Ranjbarian, S. Production of micro-and nano-composite particles by supercritical carbon dioxide. *J. Supercrit. Fluids* **40**(2), 263–283 (2007).
7. Elvassore, N. & Kikic, I. Pharmaceutical processing with supercritical fluids. In *High Pressure Process Technology: Fundamentals and Applications* (ed. Bertucco, A. G. V. G.) 612–625 (Elsevier Science, 2001).
8. Gupta, R. B. & Chattopadhyay, P Method of forming nanoparticles and microparticles of controllable size using supercritical fluids and ultrasound. *US patent No. 20020000681* (2002).
9. Reverchon, E., Adami, R., Caputo, G. & De Marco, I. Spherical microparticles production by supercritical antisolvent precipitation: Interpretation of results. *J. Supercrit. Fluids* **47**(1), 70–84 (2008).
10. Sodeifian, G., Sajadian, S. A., Ardestani, N. S. & Razmimanesh, F. Production of loratadine drug nanoparticles using ultrasonic-assisted rapid expansion of supercritical solution into aqueous solution (US-RESSAS). *J. Supercrit. Fluids* **147**, 241–253 (2019).
11. Razmimanesh, F., Sodeifian, G. & Sajadian, S. A. An investigation into Sunitinib malate nanoparticle production by US-RESOLV method: Effect of type of polymer on dissolution rate and particle size distribution. *J. Supercrit. Fluids* **170**, 105163 (2021).
12. Sodeifian, G., Sajadian, S. A. & Daneshyan, S. Preparation of Aprepitant nanoparticles (efficient drug for coping with the effects of cancer treatment) by rapid expansion of supercritical solution with solid cosolvent (RESS-SC). *J. Supercrit. Fluids* **140**, 72–84 (2018).
13. Sodeifian, G., Alwi, R. S., Razmimanesh, F. & Abadian, M. Solubility of dasatinib monohydrate (anticancer drug) in supercritical CO_2: Experimental and thermodynamic modeling. *J. Mol. Liq.* **346**, 117899 (2022).
14. Sodeifian, G., Alwi, R. S., Razmimanesh, F. & Tamura, K. Solubility of quetiapine hemifumarate (antipsychotic drug) in supercritical carbon dioxide: Experimental, modeling and hansen solubility parameter application. *Fluid Phase Equilib.* **537**, 113003 (2021).
15. Sodeifian, G., Ardestani, N. S., Sajadian, S. A. & Panah, H. S. Experimental measurements and thermodynamic modeling of Coumarin-7 solid solubility in supercritical carbon dioxide: Production of nanoparticles via RESS method. *Fluid Phase Equilib.* **483**, 122–143 (2019).
16. Sodeifian, G., Garlapati, C., Razmimanesh, F. & Ghanaat-Ghamsari, M. Measurement and modeling of clemastine fumarate (antihistamine drug) solubility in supercritical carbon dioxide. *Sci. Rep.* **11**(1), 1–16 (2021).
17. Sodeifian, G., Nasri, L., Razmimanesh, F. & Abadian, M. CO_2 utilization for determining solubility of teriflunomide (immunomodulatory agent) in supercritical carbon dioxide: Experimental investigation and thermodynamic modeling. *J. CO2 Util.* **58**, 101931 (2022).
18. Reverchon, E., Russo, P. & Stassi, A. Solubilities of solid octacosane and triacontane in supercritical carbon dioxide. *J. Chem. Eng. Data* **38**(3), 458–460 (1993).
19. Sodeifian, G., Ardestani, N. S., Sajadian, S. A. & Panah, H. S. Measurement, correlation and thermodynamic modeling of the solubility of Ketotifen fumarate (KTF) in supercritical carbon dioxide: Evaluation of PCP-SAFT equation of state. *J. Fluid Phase Equilib.* **458**, 102–114 (2018).
20. Sodeifian, G., Detakhsheshpour, R. & Sajadian, S. A. Experimental study and thermodynamic modeling of Esomeprazole (proton-pump inhibitor drug for stomach acid reduction) solubility in supercritical carbon dioxide. *J. Supercrit. Fluids* **154**, 104606 (2019).
21. Sodeifian, G., Garlapati, C., Razmimanesh, F. & Sodeifian, F. Solubility of amlodipine besylate (calcium channel blocker drug) in supercritical carbon dioxide: Measurement and correlations. *J. Chem. Eng. Data* **66**(2), 1119–1131 (2021).
22. Sodeifian, G., Garlapati, C., Razmimanesh, F. & Sodeifian, F. The solubility of Sulfabenzamide (an antibacterial drug) in supercritical carbon dioxide: Evaluation of a new thermodynamic model. *J. Mol. Liq.* **335**, 116446 (2021).
23. Sodeifian, G., Hazaveie, S. M., Sajadian, S. A. & SaadatiArdestani, N. Determination of the solubility of the repaglinide drug in supercritical carbon dioxide: experimental data and thermodynamic modeling. *J. Chem. Eng. Data* **64**(12), 5338–5348 (2019).
24. Sodeifian, G., Hsieh, C.-M., Derakhsheshpour, R., Chen, Y.-M. & Razmimanesh, F. Measurement and modeling of metoclopramide hydrochloride (anti-emetic drug) solubility in supercritical carbon dioxide. *Arab. J. Chem.* **15**, 103876 (2022).
25. Sodeifian, G., Nasri, L., Razmimanesh, F. & Abadian, M. Measuring and modeling the solubility of an antihypertensive drug (losartan potassium, Cozaar) in supercritical carbon dioxide. *J. Mol. Liq.* **331**, 115745 (2021).
26. Sodeifian, G., Razmimanesh, F., Ardestani, N. S. & Sajadian, S. A. Experimental data and thermodynamic modeling of solubility of Azathioprine, as an immunosuppressive and anti-cancer drug, in supercritical carbon dioxide. *J. Mol. Liq.* **299**, 112179 (2020).
27. Sodeifian, G., Razmimanesh, F., Sajadian, S. A. & Panah, H. S. Solubility measurement of an antihistamine drug (Loratadine) in supercritical carbon dioxide: Assessment of qCPA and PCP-SAFT equations of state. *J. Fluid Phase Equilib.* **472**, 147–159 (2018).
28. Sodeifian, G. & Sajadian, S. A. Solubility measurement and preparation of nanoparticles of an anticancer drug (Letrozole) using rapid expansion of supercritical solutions with solid cosolvent (RESS-SC). *J. Supercrit. Fluids* **133**, 239–252 (2018).
29. Sodeifian, G., Sajadian, S. A. & Razmimanesh, F. Solubility of an antiarrhythmic drug (amiodarone hydrochloride) in supercritical carbon dioxide: Experimental and modeling. *Fluid Phase Equilib.* **450**, 149–159 (2017).
30. Sodeifian, G., Sajadian, S. A., Razmimanesh, F. & Hazaveie, S. M. Solubility of Ketoconazole (antifungal drug) in $SC\text{-}CO_2$ for binary and ternary systems: Measurements and empirical correlations. *Sci. Rep.* **11**(1), 1–13 (2021).
31. Niguram, P., Polaka, S. N., Rathod, R., Kalia, K. & Kate, A. S. Update on compatibility assessment of empagliflozin with the selected pharmaceutical excipients employed in solid dosage forms by thermal, spectroscopic and chromatographic techniques. *Drug Dev. Ind. Pharm.* **46**(2), 209–218 (2020).
32. Sodeifian, G., Sajadian, S. A., Razmimanesh, F. & Ardestani, N. S. A comprehensive comparison among four different approaches for predicting the solubility of pharmaceutical solid compounds in supercritical carbon dioxide. *J. Korean J. Chem. Eng.* **35**(10), 2097–2116 (2018).
33. Bian, X.-Q., Zhang, L., Du, Z.-M., Chen, J. & Zhang, J.-Y. Prediction of sulfur solubility in supercritical sour gases using grey wolf optimizer-based support vector machine. *J. Mol. Liq.* **261**, 431–438 (2018).
34. Nguyen, H. C. *et al.* Computational prediction of drug solubility in supercritical carbon dioxide: Thermodynamic and artificial intelligence modeling. *J. Mol. Liq.* **354**, 118888 (2022).
35. Sadeghi, A. *et al.* Machine learning simulation of pharmaceutical solubility in supercritical carbon dioxide: Prediction and experimental validation for busulfan drug. *Arab. J. Chem.* **15**(1), 103502 (2022).
36. Sodeifian, G., Garlapati, C., Hazaveie, S. M. & Sodeifian, F. Solubility of 2, 4, 7-Triamino-6-phenylpteridine (triamterene, diuretic drug) in supercritical carbon dioxide: Experimental data and modeling. *J. Chem. Eng. Data* **65**(9), 4406–4416 (2020).

37. Rathnam, V. M., Lamba, N. & Madras, G. Evaluation of new density based model to correlate the solubilities of ricinoleic acid, methyl ricinoleate and methyl 10-undecenoate in supercritical carbon dioxide. *J. Supercrit. Fluids* **130**, 357–363 (2017).
38. Alwi, R. S., Garlapati, C. & Tamura, K. Solubility of anthraquinone derivatives in supercritical carbon dioxide: New correlations. *Molecules* **26**(2), 460 (2021).
39. Mahesh, G. & Garlapati, C. Modelling of solubility of some parabens in supercritical carbon dioxide and new correlations. *Arab. J. Sci. Eng.* 1–13 (2021).
40. Sodeifian, G., Razmimanesh, F. & Sajadian, S. A. Solubility measurement of a chemotherapeutic agent (Imatinib mesylate) in supercritical carbon dioxide: Assessment of new empirical model. *J. Supercrit. Fluids* **146**, 89–99 (2019).
41. Sodeifian, G., SaadatiArdestani, N., Sajadian, S. A., Golmohammadi, M. R. & Fazlali, A. Prediction of solubility of sodium valproate in supercritical carbon dioxide: Experimental study and thermodynamic modeling. *J. Chem. Eng. Data* **65**(4), 1747–1760 (2020).
42. Peper, S., Fonseca, J. M. & Dohrn, R. High-pressure fluid-phase equilibria: Trends, recent developments, and systems investigated (2009–2012). *Fluid Phase Equilib.* **484**, 126–224 (2019).
43. Alwi, R. S. & Garlapati, C. A new semi empirical model for the solubility of dyestuffs in supercritical carbon dioxide. *Chem. Pap.* **75**(6), 2585–2595 (2021).
44. Bartle, K. D., Clifford, A., Jafar, S. & Shilstone, G. Solubilities of solids and liquids of low volatility in supercritical carbon dioxide. *J. Phys. Chem. Ref. Data* **20**(4), 713–756 (1991).
45. Bian, X.-Q., Zhang, Q., Du, Z.-M., Chen, J. & Jaubert, J.-N. A five-parameter empirical model for correlating the solubility of solid compounds in supercritical carbon dioxide. *Fluid Phase Equilib.* **411**, 74–80 (2016).
46. Chrastil, J. Solubility of solids and liquids in supercritical gases. *J. Phys. Chem.* **86**(15), 3016–3021 (1982).
47. Sridar, R., Bhowal, A. & Garlapati, C. A new model for the solubility of dye compounds in supercritical carbon dioxide. *Thermochim. Acta* **561**, 91–97 (2013).
48. Garlapati, C. & Madras, G. New empirical expressions to correlate solubilities of solids in supercritical carbon dioxide. *Thermochim. Acta* **500**(1), 123–127 (2010).
49. Kumar, S. K. & Johnston, K. P. Modelling the solubility of solids in supercritical fluids with density as the independent variable. *J. Supercrit. Fluids* **1**(1), 15–22 (1988).
50. Méndez-Santiago, J. & Teja, A. S. The solubility of solids in supercritical fluids. *Fluid Phase Equilib.* **158**, 501–510 (1999).
51. Garlapati, C. & Madras, G. Solubilities of palmitic and stearic fatty acids in supercritical carbon dioxide. *J. Chem. Thermodyn.* **42**(2), 193–197 (2010).
52. Reddy, T. A. & Garlapati, C. Dimensionless empirical model to correlate pharmaceutical compound solubility in supercritical carbon dioxide. *Chem. Eng. Technol.* **42**(12), 2621–2630 (2019).
53. Huang, C.-Y., Lee, L.-S. & Su, C.-S. Correlation of solid solubilities of pharmaceutical compounds in supercritical carbon dioxide with solution model approach. *J. Taiwan Inst. Chem. Eng.* **44**(3), 349–358 (2013).
54. Iwai, Y., Koga, Y., Fukuda, T. & Arai, Y. Correlation of solubilities of high-boiling components in supercritical carbon dioxide using a solution model. *J. Chem. Eng. Jpn.* **25**(6), 757–760 (1992).
55. Kramer, A. & Thodos, G. Solubility of 1-hexadecanol and palmitic acid in supercritical carbon dioxide. *J. Chem. Eng. Data* **33**(3), 230–234 (1988).
56. Narayan, R. C., Dev, J. V. & Madras, G. Experimental determination and theoretical correlation for the solubilities of dicarboxylic acid esters in supercritical carbon dioxide. *J. Supercrit. Fluids* **101**, 87–94 (2015).
57. Nasri, L., Bensetiti, Z. & Bensaad, S. Modeling of the solubility in supercritical carbon dioxide of some solid solute isomers using the expanded liquid theory. *J. Sci. Technol.* 3(2) (2018).
58. De Zordi, N., Kikic, I., Moneghini, M. & Solinas, D. Solubility of pharmaceutical compounds in supercritical carbon dioxide. *J. Supercrit. Fluids* **66**, 16–22 (2012).
59. Garlapati, C. & Madras, G. Temperature independent mixing rules to correlate the solubilities of antibiotics and anti-inflammatory drugs in $ScCO_2$. *Thermochim. Acta* **496**(1–2), 54–58 (2009).
60. Kwak, T. & Mansoori, G. Van der Waals mixing rules for cubic equations of state. Applications for supercritical fluid extraction modelling. *Chem. Eng. Sci.* **41**(5), 1303–1309 (1986).
61. Valderrama, J. O. & Alvarez, V. H. Temperature independent mixing rules to correlate the solubility of solids in supercritical carbon dioxide. *J. Supercrit. Fluids* **32**(1–3), 37–46 (2004).
62. Fedors, R. F. A method for estimating both the solubility parameters and molar volumes of liquids. *Polym. Eng. Sci.* **14**(2), 147–154 (1974).
63. Immirzi, A. & Perini, B. Prediction of density in organic crystals. *Acta Crystallogr. Sect. A Cryst. Phys. Diffr. Theor. Gen. Crystallogr.* **33**(1), 216–218 (1977).
64. Lyman, W. J., Reehl, W. F. & Rosenblatt, D. H. *Hand Book of Chemical Property Estimation Methods* (McGraw-Hill, 1982).
65. Reid, R. C., Prausnitz, J. M. & Poling, B. E. *The Properties of Gases and Liquids*. (1987).
66. Jain, A., Yang, G. & Yalkowsky, S. H. Estimation of melting points of organic compounds. *Ind. Eng. Chem. Res.* **43**(23), 7618–7621 (2004).
67. Akaike, H. Information theory and an extension of the maximum likelihood principle. In *Proceedings of the Second International Symposium on Information Theory* (eds Petrov, B. N. & Csaki, F.) 267–281 (AkademiaaiKiado, 1973).
68. Burnham, K. P. & Anderson, D. R. Multimodel inference: Understanding AIC and BIC in model selection. *Sociol. Methods Res.* **33**(2), 261–304 (2004).
69. Deepitha, J., Pitchaiah, K., Brahmmananda Rao, C., Madras, G. & Sivaraman, N. Solubilities of dialkylhydrogen phosphonates in supercritical carbon dioxide and their correlation using semi-empirical equations. *Sep. Sci. Technol.* **54**(10), 1650–1660 (2019).
70. Kletting, P. & Glatting, G. Model selection for time-activity curves: The corrected Akaike information criterion and the F-test. *Z. Med. Phys.* **19**(3), 200–206 (2009).
71. https://webbook.nist.gov/chemistry/01 (Institute of Standards and Technology U.S. Department of Commerce, 2018).

Acknowledgements

Corresponding authors would like to thank the research deputy of university of Kashan (Grant # Pajoohaneh-1400/26) for the financial support of this project.

Author contributions

G.S. conceptualization, methodology, validation, investigation, supervision, project administration, writing—review and editing; C.G. methodology, investigation, software, writing—original draft; F.R. investigation, validation, resources; H.N. measurement.

Competing interests

The authors declare no competing interests.

Additional information

Correspondence and requests for materials should be addressed to G.S.

Reprints and permissions information is available at www.nature.com/reprints.

Publisher's note Springer Nature remains neutral with regard to jurisdictional claims in published maps and institutional affiliations.